



Acute lymphoblastic leukemia

MAPK-ERK is a central pathway in T-cell acute lymphoblastic leukemia that drives steroid resistance

Jordy C. G. van der Zwet ¹ · Jessica G. C. A. M. Buijs-Gladdines¹ · Valentina Cordo' ¹ · Donna O. Debets² · Willem K. Smits¹ · Zhongli Chen¹ · Jelle Dylus³ · Guido J. R. Zaman³ · Maarten Altelaar² · Koichi Oshima⁴ · Beat Bornhauser ⁵ · Jean-Pierre Bourquin⁵ · Jan Cools ⁶ · Adolfo A. Ferrando ⁴ · Josef Vormoor ^{1,7} · Rob Pieters¹ · Britta Vormoor¹ · Jules P. P. Meijerink ¹

Received: 28 October 2020 / Revised: 17 April 2021 / Accepted: 7 May 2021 / Published online: 18 May 2021
© The Author(s), under exclusive licence to Springer Nature Limited 2021

Abstract

(Patho-)physiological activation of the IL7-receptor (IL7R) signaling contributes to steroid resistance in pediatric T-cell acute lymphoblastic leukemia (T-ALL). Here, we show that activating IL7R pathway mutations and physiological IL7R signaling activate MAPK-ERK signaling, which provokes steroid resistance by phosphorylation of BIM. By mass spectrometry, we demonstrate that phosphorylated BIM is impaired in binding to BCL2, BCLXL and MCL1, shifting the apoptotic balance toward survival. Treatment with MEK inhibitors abolishes this inactivating phosphorylation of BIM and restores its interaction with anti-apoptotic BCL2-protein family members. Importantly, the MEK inhibitor selumetinib synergizes with steroids in both IL7-dependent and IL7-independent steroid resistant pediatric T-ALL PDX samples. Despite the anti-MAPK-ERK activity of ruxolitinib in IL7-induced signaling and JAK1 mutant cells, ruxolitinib only synergizes with steroid treatment in IL7-dependent steroid resistant PDX samples but not in IL7-independent steroid resistant PDX samples. Our study highlights the central role for MAPK-ERK signaling in steroid resistance in T-ALL patients, and demonstrates the broader application of MEK inhibitors over ruxolitinib to resensitize steroid-resistant T-ALL cells. These findings strongly support the enrollment of T-ALL patients in the current phase I/II SeluDex trial (NCT03705507) and contributes to the optimization and stratification of newly designed T-ALL treatment regimens.

Supplementary information The online version contains supplementary material available at <https://doi.org/10.1038/s41375-021-01291-5>.

✉ Jules P. P. Meijerink
j.meijerink@prinsesmaximacentrum.nl

- ¹ Princess Máxima Center for Pediatric Oncology, Utrecht, the Netherlands
- ² Biomolecular Mass Spectrometry and Proteomics, Bijvoet Center of Biomolecular Research and Utrecht Institute for Pharmaceutical Sciences, Utrecht University, Utrecht, the Netherlands
- ³ Netherlands Translational Research Center B.V., Oss, the Netherlands
- ⁴ Institute of Cancer Genetics, Columbia University Medical Center, New York, NY, USA
- ⁵ Children's Research Center, University Children's Hospital Zurich, Zurich, Switzerland
- ⁶ KU Leuven Center for Human Genetics & VIB Center for Cancer Biology, Leuven, Belgium
- ⁷ Newcastle University, Newcastle upon Tyne, UK

Introduction

T-cell acute lymphoblastic leukemia (T-ALL) is a high-risk hematological malignancy of early developing T-cells and represents 15% of children that present with ALL. T-ALL patients comprised nearly 40% of patients that were treated in the high-risk treatment arm of the Dutch Childhood Oncology Group (DCOG) ALL-10 protocol [1]. To date, cure-rates of 75–80% are achieved [2–4], indicating that therapy still fails in one out of 4–5 children with T-ALL. T-ALL patients that suffer from relapse have a dismal outcome due to acquired resistance to a wide range of chemotherapeutics. Synthetic glucocorticoids (also denoted as steroids) including prednisolone and dexamethasone are cornerstone drugs in the treatment of both T-ALL and B-cell precursor-ALL (BCP-ALL). Resistance to steroids is a frequent problem in T-ALL that historically predicts for poor outcome and is used for risk-stratification in many treatment protocols including the DCOG ALL-11

protocol [3, 5, 6]. The gene coding for the pro-apoptotic molecule BIM [7]—a BH3-only member of the BCL-2 protein family—is an important direct transcriptional target of the glucocorticoid receptor (NR3C1). Upon steroid treatment, BIM is upregulated to mediate steroid-induced death of lymphoid cells [8–12]. In contrast, anti-apoptotic BCL2 is downregulated in lymphoblasts treated with steroids [8]. Upregulation of BIM changes the dynamic balance between pro- and anti-apoptotic BCL-2 family members, resulting in the release and activation of the pro-apoptotic effector molecules BAK and BAX, which triggers apoptosis [13–15]. Various mechanisms have been described that may impair the activation or function of BIM, hence resulting in steroid resistance. These mechanisms rely on the activation of specific kinases (e.g., AKT, ERK, p38 or JNK) that can either impair the transcription of *BIM*, or alter its function, cellular localization and/or proteasomal degradation [10, 11, 16–24]. Aberrant activation of the interleukin-7 (IL7) signaling pathway is frequently observed in T-ALL [25–27]. Physiological activation of the pathway is induced when IL7 binds to its cognate receptor, which results in the activation of downstream JAK-STAT and PI3K-AKT pathways. We previously demonstrated that mutations in the IL7R signaling pathway are associated with steroid resistance and inferior relapse-free survival [28]. Mutations in the IL7R α chain or downstream signaling molecules activate the JAK-STAT and PI3K-AKT signaling pathways in a ligand-independent manner [28]. In contrast to physiological IL7R signaling in normal T-cells, IL7R-signaling mutations also strongly activate MAPK-ERK signaling, albeit its significance is currently unknown. Physiological IL7R signaling in T-ALL cells from patients can also raise steroid resistance, further providing evidence for crosstalk between the IL7- and steroid-induced signaling pathways independent of the presence of specific activation mutations [29]. To date, this so-called ‘IL7-dependent steroid resistant’ phenotype is attributed to STAT5 activation and subsequent upregulation of *BCL2* [30]. *BCL2* upregulation also occurs as a result of IL7-induced PI3K-AKT pathway activation in T-ALL [25]. However, the activation of the MAPK-ERK pathway in IL7-induced signaling in T-ALL has not been studied yet, and its contribution to steroid resistance remains poorly understood. This study reveals that the MAPK-ERK pathway is aberrantly activated downstream of mutant- and physiological IL7R-signaling. As a result, steroid-induced pro-apoptotic BIM is inactivated through phosphorylation, which changes the apoptotic threshold and drives MAPK-ERK induced steroid resistance. Our results demonstrate the broader efficacy of MEK inhibitors over the JAK1/2-inhibitor ruxolitinib to resensitize steroid-resistant T-ALL cells.

Materials and methods

Functional screening of SUPT-1 cell lines

JAK1, IL7R, and NRAS mutant or wild-type molecules were stably expressed through lentiviral transduction of SUPT-1 cells. Viability during cytotoxicity screens was determined after 4 days by methylthiazolyldiphenyl-tetrazolium bromide (MTT, Sigma Aldrich). Details concerning lentiviral transduction and purification of cell lines, cytotoxicity screens and RTQ-PCR can be found in the supplementary materials and methods.

Functional screening of PDX cells

Cytotoxicity screens of PDX samples was performed as previously described [28] in the presence or absence of 25 ng/ml IL7 (R&D Systems). PDX cells were plated at a concentration of 1×10^6 cells/ml, and viability after 4 days was measured by ATPlite 1Step (Perkin Elmer, Groningen, The Netherlands).

Co-immuno-precipitation and mass spectrometry

Dynabeads (Thermo Fisher Scientific) were linked to the immunoprecipitation antibody of interest, briefly incubated and subsequently crosslinked to BS³ (2.5 mM) to avoid co-elution of the antibody. After overnight incubation each sample was eluted with Laemmli sample buffer (without dithiothreitol) and heated for 10' at 50 °C. Antibodies used for immunoprecipitation of target proteins: BIM (#2933; Cell Signaling), MCL1 (#AHO0102; Thermo Fisher Scientific) and BCL2 (#551051; BD PharmingenTM). For mass spectrometry, proteins were digested by trypsin (Promega) and peptides were analyzed by LC-MS/MS using an Agilent 1290 system coupled to a Q-exactive HF-X (Thermo Fisher Scientific). iBAQ quantification was performed, representing protein abundance in each sample. Details concerning protein isolation in non-IP experiments, the western-blotting procedure and mass spectrometry procedures and analysis can be found in the supplementary materials and methods.

Results

Steroid resistant IL7R and JAK1 mutants activate the MAPK-ERK signaling pathway

To explore the mechanisms driving IL7R-signaling mediated steroid resistance, we generated doxycycline-inducible SUPT-1 cell lines that express wild-type or mutant IL7R or downstream signaling components. Whereas expression of wild-type IL7R (IL7R^{WT}) or the non-cysteine mutant

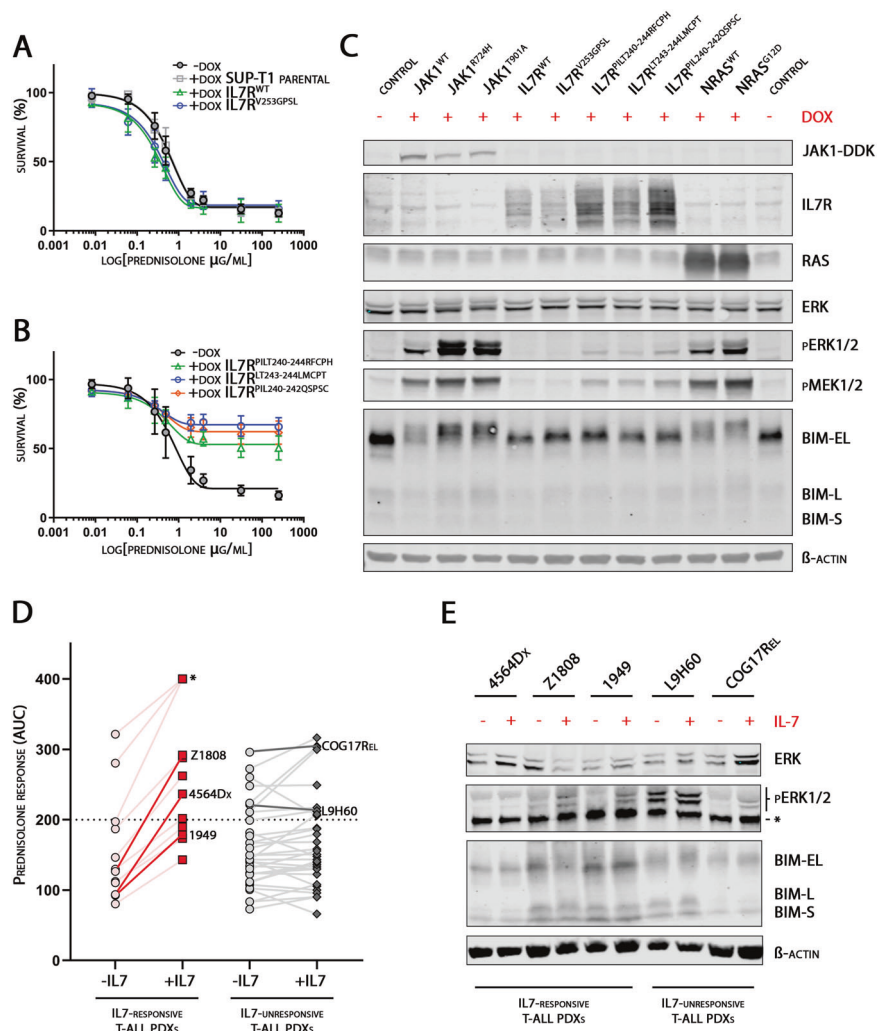


Fig. 1 IL7R signaling mutations and physiological IL7-signaling activates MAPK-ERK signaling in T-ALL. **A** Cell toxicity screening of doxycycline-induced SUPT-1 parental (gray), IL7R^{WT} (green) and IL7R^{V253GPSL} (blue) mutant cells. As negative control for the mutant cell lines, the average survival of both cell lines is illustrated in the -DOX condition (dark gray). Cells were treated with prednisolone (range 0.00822–250 µg/ml) for 4 days. **B** Cell toxicity screening of doxycycline-induced IL7R^{PILT240-244RFCPH} (green), IL7R^{LT243-244LMCPT} (blue) and IL7R^{PIL240-242QSPSC} (orange) cysteine-mutant cells. As negative control for the mutant cell lines, the average survival of both cell lines is illustrated in the -DOX condition (dark gray). Cells were treated with prednisolone (range 0.00822–250 µg/ml) for 4 days. **C**

Western blot of JAK1 (DDK-tagged), IL7R and NRAS overexpressing cells to study downstream MAPK-ERK pathway activation. **D** Cell toxicity screening of 46 T-ALL PDX samples in IL7 treated and untreated condition. Area Under the Curve (AUC) values represent steroid response (range 3.16–31.6 µM prednisolone). The ‘IL7-responsive’ group was defined by an >1.5 fold increase in prednisolone AUC in the IL7 treated condition. Starred samples represent extreme resistant samples with AUC > 400, since an AUC of 400 represent the maximum AUC in a 4-log dynamic concentration range of prednisolone. **E** Western blot of selected T-ALL PDX samples to study downstream MAPK-ERK pathway activation in response to IL7. *off-target band.

IL7R^{V253GPSL} did not affect the sensitive steroid response of SUPT-1 cells, expression of cysteine mutant IL7R^{PILT240-244RFCPH}, IL7R^{PIL240-242QSPSC} or IL7R^{LT243-244LMCPT} strongly raised cellular resistance (Fig. 1A, B). We observed activation of the downstream MAPK-ERK signaling in these three steroid resistant lines expressing mutant IL7R α isoforms in contrast to the wild-type and the non-cysteine IL7R α mutant lines (Fig. 1C). Notably, MAPK-ERK activation has not been observed in

physiological IL7 signaling in normal T-cells [31]. Validation of MAPK-ERK activation in other steroid sensitive (JAK1^{WT}) or steroid resistant (JAK1^{R724H}, JAK1^{T901A}, NRAS^{WT} or NRAS^{G12D}) derivate SUPT-1 lines demonstrated strong MAPK-ERK activation in all steroid resistant lines [28]. As the inducibility of all doxycycline-inducible cell lines exceeded 85% (data not shown), differences in MAPK-ERK signaling among various cell lines reflect quantitative differences. Of note, MAPK-ERK

pathway activation seemed linked to changes in the apparent molecular weight of the pro-apoptotic BIM-EL and BIM-L isoforms (Fig. 1C). Changes in the apparent molecular weight of the pro-apoptotic BIM-S isoform was not observed.

IL7 can induce steroid resistance and MAPK-ERK activation in T-ALL PDX cells

Our observed relationship between mutant IL7R signaling, MAPK-ERK pathway activation and steroid response suggests that MAPK-ERK signaling may represent a major determinant for steroid resistance, including steroid resistance that is induced by physiological IL7 signaling. We therefore examined the steroid response of 46 patient-derived xenografts (PDX) samples (including nine matched diagnostic-relapse PDX pairs) in the absence and presence of IL7. Steroid sensitivity was measured as Area Under the Curve (AUC) to quantify cytotoxic responses over a 4-log dynamic range of prednisolone concentrations. The steroid sensitivity of 34 PDX samples was not affected by addition of IL7. However, 12 samples demonstrated an AUC increase of more than 1.5-fold in the presence of IL7 compared to cells cultured in the absence of IL7 (Fig. 1D, Supplementary Fig. 1a). This indicates that ligand-dependent IL7R activation can induce steroid resistance in 26% of our T-ALL PDX cohort. We then studied whether IL7-induced signaling can activate the MAPK-ERK pathway alike IL7R signaling mutations. For this, we selected three PDX samples that became more resistant to steroids following IL7 exposure (denoted as IL7-dependent steroid resistant samples), and two steroid resistant PDX samples for which the steroid sensitivity was not affected by IL7 (denoted as IL7-independent steroid resistant samples) (Supplementary Fig. 1b, c). Interestingly, we observed increased ERK phosphorylation after 30 min of IL7 exposure in IL7-dependent and IL7-independent steroid resistant PDX samples (Fig. 1E, Supplementary Fig. 1d). In some of these samples, higher molecular weight isoforms of BIM-L and BIM-EL were observed in relation to (IL7-induced) MAPK-ERK signaling. In addition to mutant IL7R signaling, we reveal that physiological IL7 signaling also activates the MAPK-ERK pathway in T-ALL. MAPK-ERK signaling may therefore represent a major cause for IL7-induced steroid resistance.

MAPK-ERK signaling drives phosphorylation of BIM isoforms

The presence of higher molecular weight BIM-EL and BIM-L isoforms in MAPK-ERK activated and steroid resistant cell lines and T-ALL PDX samples suggest a common post-translational modification of BIM

downstream of activated MAPK-ERK signaling. To study if this modification was due to protein phosphorylation, we treated whole cell lysates of doxycycline-induced SUPT-1 JAK1^{R724H} cells ex-vivo with lambda phosphatase in the presence of limiting concentrations of phosphatase inhibitors. Induction of JAK1^{R724H} resulted in high phosphorylation of ERK and higher molecular weight forms for BIM-EL and BIM-L, which were reduced to single and lower molecular isoforms upon phosphatase treatment similar to non-induced control cells (Fig. 2A, only BIM-EL isoform is displayed). Therefore, we conclude that these higher molecular weight BIM isoforms were due to phosphorylation. To investigate whether BIM is phosphorylated downstream of activated MAPK-ERK signaling, we performed an in-vitro phosphorylation assay with human active (MEK-activated) recombinant ERK1 and human recombinant BIM-L (Fig. 2B). Only in the presence of ERK1 and 100 μ M ATP, BIM was phosphorylated, concluding that ERK is directly responsible for the phosphorylation of pro-apoptotic BIM. We validated this result by treating wild-type and mutant JAK1 SUPT-1 cells with the MEK-inhibitor CI1040 (Fig. 2C). In both JAK mutated lines, phosphorylation of ERK and BIM-EL and BIM-L isoforms were effectively blocked upon CI1040 treatment. Similar findings were observed for three cysteine-mutant IL7R α lines following CI1040 treatment, while BIM remained unphosphorylated in wild-type IL7R α cells irrespective of MEK inhibitor treatment (Supplementary Fig. 2a). Both clinically relevant MEK inhibitors selumetinib and trametinib also effectively blocked BIM phosphorylation in a dose-dependent manner at concentrations that did not induce cytotoxicity (Fig. 2D, E, Supplementary Fig. 2b–d). Therefore, we conclude that phosphorylation of BIM follows MAPK-ERK pathway activation and can be effectively blocked by MEK inhibitors.

The transcriptional steroid response is intact in SUPT-1 steroid resistant lines

BIM, among other genes, represents an important transcriptional target gene of the glucocorticoid receptor (NR3C1) [8–10, 12, 18, 21, 32]. Failure to upregulate *BIM* has been linked to steroid resistance in pediatric ALL patients and ALL PDX samples [8, 17, 18, 33]. To establish whether transcriptional activation of *BIM* is impaired as a potential steroid resistance mechanism downstream of mutant IL7R signaling, we measured *BIM* expression in the presence and absence of steroid treatment in SUPT-1 cells with and without expression of mutant JAK1 or IL7R α molecules (Fig. 3A, B). In the absence of doxycycline, where cells do not express mutant molecules (i.e., steroid sensitive phenotype), all cell lines underwent a 4- to 10-fold

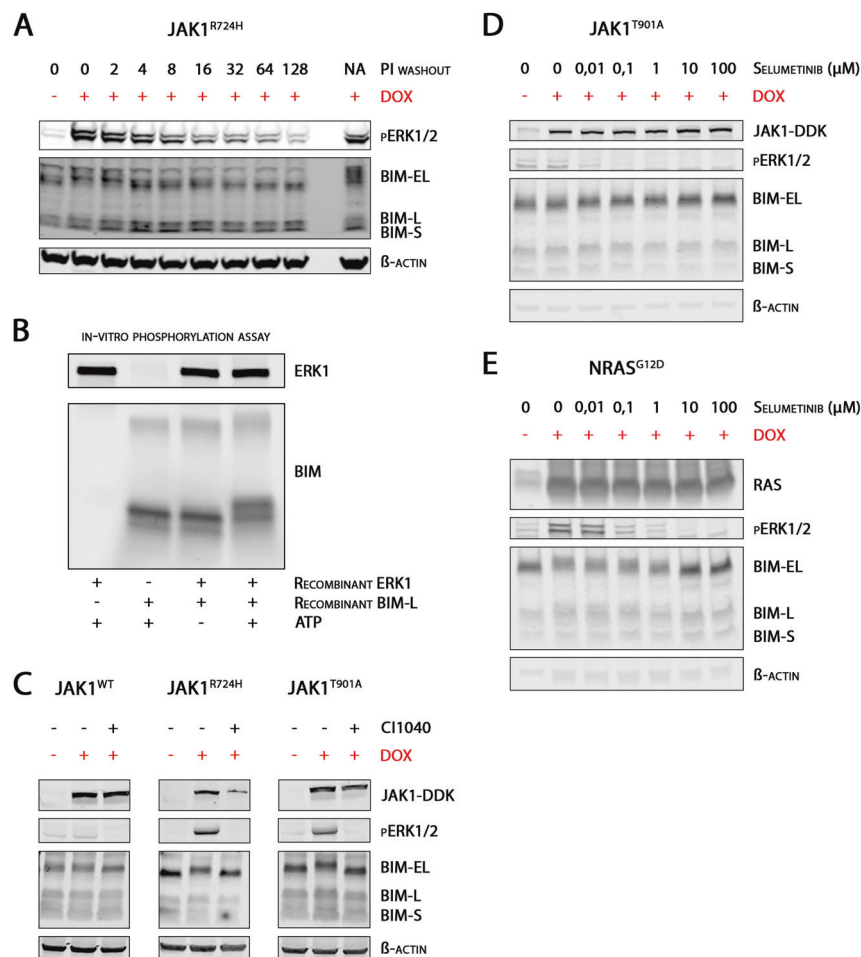


Fig. 2 Pro-apoptotic BIM is phosphorylated downstream of activated MAPK-ERK signaling. **A** Western blot of JAK1^{R724H} over-expressing cells (+DOX) treated with lambda phosphatase during cell lysis. A standard phosphatase inhibitor (PI) cocktail used for cell lysis was diluted 0–128 times to study the effect of lambda phosphatase in absence of phosphatase inhibitors. A lambda phosphatase untreated sample with standard PI cocktail levels (last lane, PI dilution ‘NA’) was used as a control. **B** In-vitro phosphorylation assay between

recombinant ERK1 and BIM-L in a 1:3 kinase: substrate weight ratio. The kinase reaction was performed in the presence and absence of 100 μM ATP (lane 1, 3 and 4). **C** Western blot of wild-type and mutant JAK1 cells that were induced (second lane in each individual blot) and treated with 2 μM of MEK inhibitor CI1040 (third lane in each individual blot). **D** and **E** Protein phosphorylation of ERK and BIM at increasing concentration of MEK inhibitor selumetinib (range 0–100 μM) in JAK1^{T901A} and NRAS^{G12D} overexpressing cells.

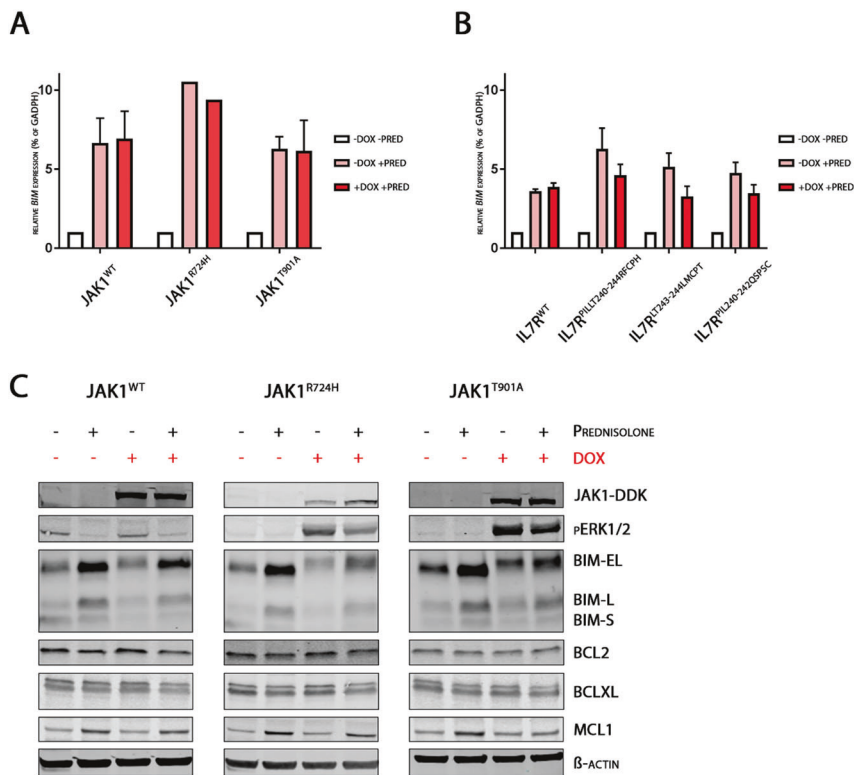
increase in *BIM* expression following overnight exposure to prednisolone. Doxycycline-induced expression of mutant (and steroid resistant) JAK1 or IL7Rα molecules also resulted in a robust upregulation of *BIM* following steroid treatment. This was also confirmed at the protein level, where steroid treatment led to increased BIM levels independently of MAPK-ERK signaling (Fig. 3C). This indicates that the transcriptional response of NR3C1 upon steroid exposure remains intact in steroid resistant IL7R and JAK1 mutant lines, which hints that phosphorylation of BIM may drive MAPK-ERK-dependent steroid resistance. Notably, *MCL1* levels also increased following prednisolone exposure in all lines tested, indicating that *MCL1* might represent a novel and direct transcriptional target gene of NR3C1 (Fig. 3C).

Phosphorylation of BIM impairs its binding to anti-apoptotic BCL-2 family members

BIM can bind to anti-apoptotic family members including BCL2, BCLW, BCLXL and MCL1 to antagonize their pro-survival activities [7, 34–37]. We hypothesized that phosphorylation of BIM is causative for MAPK-ERK dependent steroid resistance in T-ALL by directly impairing the binding of BIM to anti-apoptotic family members. We therefore performed a qualitative unbiased mass spectrometry analysis of BIM-immunoprecipitation eluates from non-induced and doxycycline-induced NRAS^{G12D} cells. As a result, we identified 23 proteins that consistently bound to unphosphorylated BIM in three replicate experiments (Supplementary Table 1). Between eluates, we observed

Fig. 3 Steroid-dependent expression of *BIM* is not impaired in MAPK-ERK activated cell lines. A–B

Relative *BIM* expression levels (mean and SD of triplicates) of wild-type and mutant JAK1 and IL7R cell lines. Expression was normalized to *GAPDH* expression. *BIM* expression of non-induced cells that were not treated with prednisolone was used as baseline (relative expression = 1). RT-QPCR was performed on both doxycycline-induced and non-induced samples that were treated overnight with prednisolone (250 µg/ml). **C** Pathway signaling and BH3-protein family members were studied in steroid-treated (250 µg/ml prednisolone) and untreated wild-type and mutant JAK1 cells.



variation in BIM protein abundance (quantified by the BIM iBAQ value; Supplementary Fig. 3a, Supplementary Table 1). This variation could easily be explained by differences in immunoprecipitation efficiency, but could also be caused by potential proteasomal degradation of phosphorylated BIM [11, 22, 23]. By treating NRAS^{G12D} over-expressing cells with the proteasomal inhibitor bortezomib, we indeed observed moderate increased BIM protein levels, whereas MCL1 stabilization confirmed effective inhibition of the proteasome (Supplementary Fig. 3b). To correct our analysis for technical differences and proteasomal degradation, we normalized the iBAQ value of each individual protein to the BIM iBAQ value within each sample (Supplementary Table 1). Since the *BIM* gene is a direct target gene of the glucocorticoid receptor, mass spectrometry and subsequent normalization was also performed on BIM-immunoprecipitation eluates of prednisolone-treated NRAS^{G12D} cells. This qualitative mass spectrometry approach demonstrated that five out of 23 proteins consistently decreased direct protein-protein interaction with BIM upon its phosphorylation (Fig. 4A, Supplementary Table 1). With the exception of Aurora Kinase A (AURKA), the other four proteins represent BCL-2-family members, that is BCLXL, BCL2, MCL1 and BMF.

To validate the finding that phosphorylation impairs the capability of BIM to bind anti-apoptotic BCL-2 family members, we performed BIM-immunoprecipitation in

steroid-sensitive (JAK1^{WT}) and steroid-resistant (JAK1^{T901A}, JAK1^{R724H} and the NRAS^{G12D}) cell lines (Fig. 4B–C, Supplementary Fig. 4a, b). As expected, (non-phosphorylated) BIM effectively binds MCL1, BCL2 and BCLXL in all these lines under non-induced, steroid-sensitive conditions. Moreover, steroid-dependent BIM upregulation further enhanced capturing of MCL1, BCL2 and BCLXL proteins (lane 5 and 6). Following doxycycline-induced expression of mutant JAK1 or NRAS molecules and subsequent BIM phosphorylation, BIM decreased its binding to all three anti-apoptotic molecules (compare lanes 7 and 8 to 5 and 6, respectively). Reciprocal immunoprecipitation experiments for BCL2 or MCL1 using the NRAS^{G12D} line also confirmed reduced binding to BIM isoforms following BIM phosphorylation (Supplementary Fig. 4c, d). We therefore conclude that phosphorylation of BIM impairs its interaction with anti-apoptotic BCL-2 family members, which drives steroid resistance. Following inhibition of the proteasome, which slightly elevated BIM protein levels, we did not observe enhanced binding of BIM to BCL2 (Supplementary Fig. 4e). This confirms that phosphorylation of BIM results in loss-of-binding to anti-apoptotic molecules, rather than indirectly due to proteasomal degradation. Unfortunately, we were unable to identify the BIM phospho-motif responsible for this loss-of-binding effect, since phosphorylation at known Ser55, Ser69, Thr56 and Thr112 was not observed in our SUPT-1

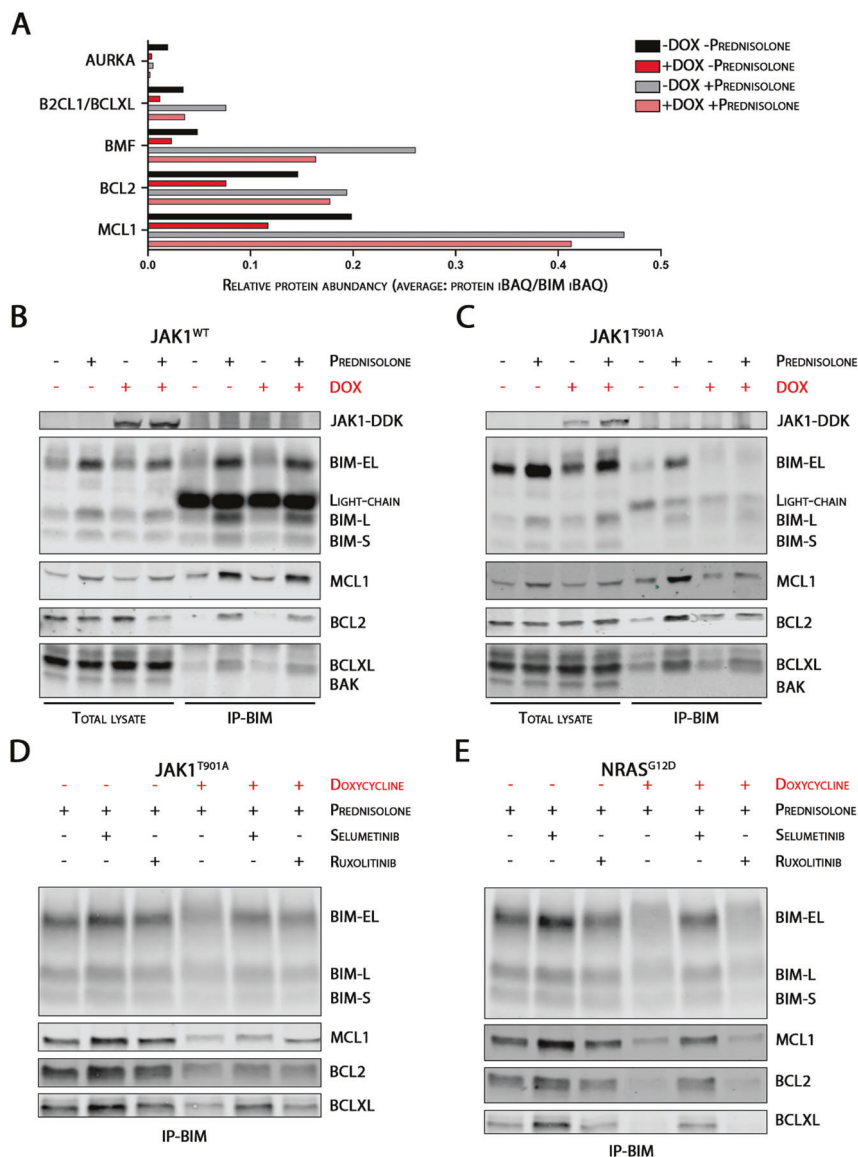


Fig. 4 Phosphorylation of BIM directly impairs its binding to anti-apoptotic proteins, which is prevented by pharmacological inhibition of MAPK-ERK signaling. **A** Protein abundance of five proteins identified by qualitative mass spectrometry that lost binding to BIM upon BIM phosphorylation in prednisolone untreated and treated conditions. Relative protein abundance was determined by the ratio of protein abundance in each individual sample (protein iBAQ) versus total BIM protein abundance in each individual sample (BIM iBAQ). Bars represent the average of the replicates ($n=3$) in NRAS^{G12D} SUPT-1 cells. The comparison between -dox -prednisolone versus +dox -prednisolone and -dox +prednisolone versus +dox +prednisolone illustrate the loss-of-binding of these five proteins. Samples were induced by doxycycline and/or treated with 250 μ g/ml

prednisolone for 24 h before BIM immunoprecipitation. **B–C** BIM-immunoprecipitation of wild-type JAK1 and JAK1^{T901A} mutant cells. Lane 1–4: total lysate of induced and non-induced cells incubated overnight in the absence or presence of 250 μ g/ml prednisolone. Lane 5–6: BIM-immunoprecipitation of corresponding samples, studying differences in the binding of BIM to anti-apoptotic BCL2 family members (MCL1, BCL2 and BCLXL). **D–E** BIM-immunoprecipitation of JAK1^{T901A} and NRAS^{G12D} mutant cells. In addition to doxycycline-induction and prednisolone treatment (250 μ g/ml prednisolone), samples were treated with either 2 μ M ruxolitinib or 10 μ M selumetinib. Corresponding total lysate blots are presented in Supplementary Fig. 4a, b.

cell lines with activated MAPK-ERK signaling (data not shown).

To explore therapeutic options for this MAPK-ERK-induced steroid resistance mechanism, we studied to what extent JAK or MEK inhibitors are able to prevent phosphorylation of BIM and to restore its binding to anti-

apoptotic family members. For this, BIM was precipitated in lysates from doxycycline-induced JAK1^{T901A} and NRAS^{G12D} lines that were treated with the JAK1/2-inhibitor ruxolitinib or the MEK inhibitor selumetinib. Treatment with either ruxolitinib or selumetinib abolished MAPK-ERK and consequential phosphorylation of BIM in JAK1

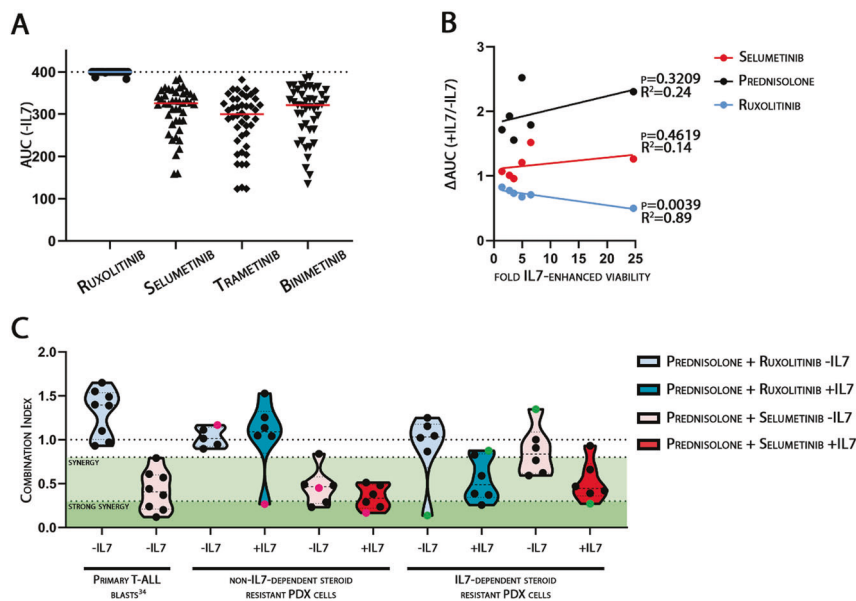


Fig. 5 MEK-inhibitors synergize with steroid treatment in IL7-dependent and IL7-independent steroid-resistant T-ALL. **A** Cell toxicity screening of 46 T-ALL PDX samples for ruxolitinib (JAK-inhibitor), selumetinib, trametinib or binimetinib (MEK inhibitors) in IL7 untreated condition. Cell viability is illustrated by AUC, whereas an AUC of 400 represent the maximum AUC in a 4-log dynamic concentration range of each specific inhibitor. **B** Correlation between IL7-enhanced cell viability and altered drug sensitivity in the presence of IL7 in six ‘IL7-dependent steroid resistant’ PDX samples. ‘IL7-dependent steroid resistant’ PDX samples were defined by an increase in prednisolone AUC by >1.5 fold in the presence of IL7 with a minimal AUC of 175 in the presence of IL7. Y-axis represent delta AUC, defined by the ratio between the AUC of the specific drug in the

presence and absence of IL7. X-axis represent the magnitude of IL7-enhanced viability in each individual sample relative to viability in the absence of IL7 (Supplementary Fig. 5a). Linear regression (R^2) and p values conclude a significant correlation between IL7-enhanced viability and ruxolitinib sensitivity. **C** The combination Index (CI) of T-ALL PDX samples, treated with prednisolone and ruxolitinib (blue) or selumetinib (red) treatment in the absence (light colored) or presence (dark colored) of IL7. The synergy value of each sample illustrated is an average CI score, calculated over the complete therapeutic window of the combination treatment (Supplementary Fig. 6a, b). Synergy was defined by a CI between 0.3 and 0.8, whereas strong synergy was defined by a CI < 0.3. PDX COG17 was highlighted by the purple dots, whereas PDX Z1808 was highlighted by the green dots.

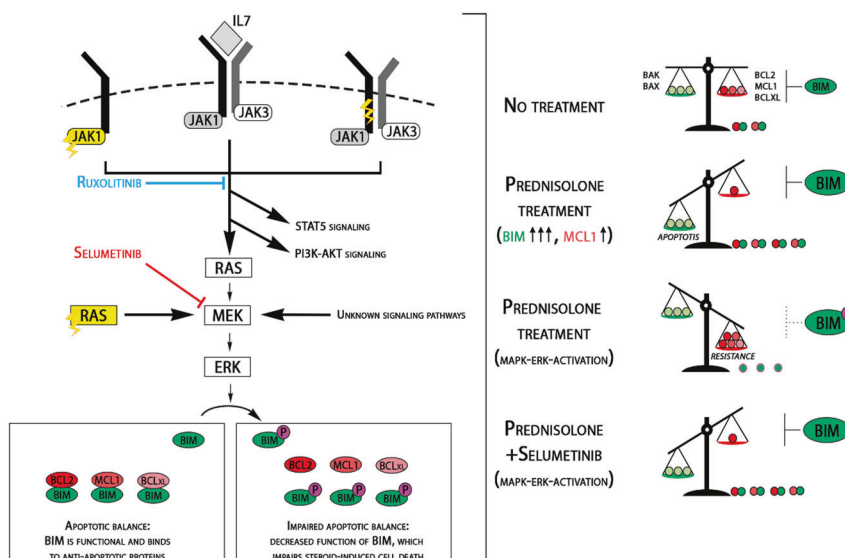
mutant cells, whereas the effect of selumetinib was independent on active JAK1 signaling (Supplementary Fig. 5a; lanes 5 and 6). As expected, selumetinib but not ruxolitinib abolished MAPK-ERK activation and subsequent phosphorylation of BIM in doxycycline-induced NRAS^{G12D} cells (Supplementary Fig. 5b; lanes 5 and 6). Restoration of non-phosphorylated BIM in both lines restored its binding to MCL1, BCL2 and BCLXL (Fig. 4D, E, lanes 4, 5 and 6). Treatment with selumetinib or ruxolitinib also prevented phosphorylation of BIM upon IL7 exposure in the T-ALL PDX sample Z1808 (Supplementary Fig. 5c). We therefore conclude that the adverse effects of MAPK-ERK pathway activation downstream of active IL7R/JAK signaling can be blocked by both JAK and MEK inhibitors, while MAPK-ERK activation by mutations downstream of the IL7R or JAK molecules can only be blocked by MEK inhibitors.

MEK-ERK inhibition enhances steroid responsiveness

To elaborate on the clinical application of these targeted compounds in T-ALL, we first tested the cytotoxic efficacy

of ruxolitinib or MEK inhibitors selumetinib, trametinib and binimetinib in 46 T-ALL PDX samples. In the absence of IL7, none of the PDX samples tested responded to single ruxolitinib treatment, while the majority of these samples demonstrated a robust response to all three MEK inhibitors (Fig. 5A). Since ruxolitinib seems effective in PDX-models when tested in-vivo [29, 38], we hypothesized that its therapeutic effect may be dependent on IL7-enhanced survival and/or proliferation pathways. We therefore studied the relationship between IL7-dependent viability and ruxolitinib sensitivity in six IL7-dependent steroid resistant PDX samples (Supplementary Fig. 6a). These PDX cells were more viable when cultured in the presence of IL7 (Supplementary Table 2), and became sensitive to ruxolitinib treatment (Supplementary Fig. 6a). Importantly, we observed a significant correlation ($p = 0.0039$) between increased ruxolitinib sensitivity and the level of IL7-enhanced viability (Fig. 5B, Supplementary Fig. 6a). This was not observed for six IL7-independent steroid resistant PDX samples that remained insensitive to ruxolitinib even in the presence of IL7 (Supplementary Table 2, Supplementary Fig. 6b). Therefore, we conclude that the

Fig. 6 Schematic overview of MAPK-ERK-induced steroid resistance. Cysteine IL7R α mutations, JAK1 mutations, and physiological IL7 signaling can activate the MAPK-ERK signaling pathway in T-ALL. In addition, the MAPK-ERK pathway can be activated by RAS mutations or unknown (i.e., non-IL7) signaling pathways. Activated ERK phosphorylates the pro-apoptotic molecule BIM, which normally binds to anti-apoptotic Bcl-2 family proteins (BCL2, BCLXL and MCL1).



therapeutic effect of ruxolitinib is dependent on IL7-enhanced cell viability. This may limit the therapeutic application of ruxolitinib, since only a minority of T-ALLs exploit IL7-signaling to provoke steroid resistance (Fig. 1D). Cellular sensitivity toward selumetinib was independent on IL7-enhanced viability (Fig. 5B, Supplementary Fig. 6a).

We then investigated whether pharmacological inhibition of MAPK-ERK signaling could synergize with prednisolone in steroid-resistant T-ALL cells. For this, we combined prednisolone treatment with selumetinib or ruxolitinib in the six IL7-independent steroid-resistant PDX samples and the six IL7-dependent steroid resistant PDX samples (Fig. 5C, supplementary Fig. 7a, b, supplementary Table 3). Combination treatment with prednisolone and selumetinib was highly synergistic in both IL7-dependent and IL7-independent steroid resistant samples. This highlights that MAPK-ERK signaling is a central driver in both IL7-dependent and IL7-independent steroid resistance mechanisms in T-ALL. Selumetinib was also synergistic in PDX cells under steroid-sensitive conditions (e.g., IL7-dependent cells that were tested in the absence of IL7). In addition to all IL7-dependent steroid resistant samples, only one IL7-independent steroid resistant sample demonstrated synergy between prednisolone and ruxolitinib in the presence of IL7 (PDX COG17R, purple dots, Fig. 5C). Interestingly, synergy between prednisolone and ruxolitinib was also observed in one IL7-dependent steroid resistant sample in the absence of IL7 (PDX Z1808, green dots, Fig. 5C). For both samples in their respective conditions, we did observe STAT5 activation and subsequent BCL2 upregulation (Supplementary Fig. 1b). However, both samples also heavily benefitted from combined prednisolone and selumetinib treatment (– or + IL7 lanes for PDX COG17R, +

IL7 lane for PDX Z1808). Therefore, these results highlight that MEK inhibitors are superior over the JAK1/2-inhibitor ruxolitinib, since MEK-inhibitors can resensitize steroid-resistant T-ALL patients that are insensitive to ruxolitinib treatment.

Discussion

In the last two decades, major improvements have been made in the treatment of pediatric T-ALL. Certain genetic aberrations, like recurrent IL7R pathway mutations, are related to drug resistance and inferior outcome [28, 39, 40]. Here, we demonstrate that both ligand- and mutation-induced IL7R signaling activates the MAPK-ERK pathway in cell lines and pediatric T-ALL PDX samples. Activated MEK-ERK phosphorylates pro-apoptotic BIM, which impairs its binding to anti-apoptotic proteins, resulting in steroid resistance. We demonstrate that MEK inhibitors effectively abolish this resistance mechanism and synergize with steroid treatment (Fig. 6). These data highlight an opportunity for treatment with MEK inhibitors in MAPK-ERK activated T-ALL during steroid therapy. Moreover, treatment with MEK inhibitors could prevent selection of cells that harbor MAPK-ERK-activating mutations during steroid treatment. The latter specifically accounts for *IL7Ra*, *JAK1* and *NRAS* mutations [28], especially since *IL7Ra* and *NRAS* mutations have been identified as predictors for extremely poor outcome for relapsed T-ALL patients [41]. Interestingly, we observed synergy between MEK inhibitor selumetinib and prednisolone in both IL7-dependent and IL7-independent PDX samples. This implies that the application of MEK inhibitors in T-ALL is not limited to specific T-ALL patient subgroups or certain genetic

aberrations, but that the MAPK-ERK pathway may be a central convergence point that is activated downstream of multiple important signaling pathways in T-ALL.

MAPK-ERK activation induces phosphorylation of BIM-EL and BIM-L isoforms. BIM-EL consists of exons 2-6, with exon 3 containing at least three serine residues (Ser-59, Ser-69 and Ser-77) that are known sites for phosphorylation by ERK [11, 22, 42]. Although BIM-L lacks exon 3, we observed that this isoform is also subjected to phosphorylation that can be abolished by MEK inhibitor treatment. Phosphorylation of the pro-apoptotic BIM-S isoform, which only consists of exons 5 and 6, was not observed in our models. Therefore, we predict that one or multiple residues on BIM exon 4 can also be subjected to ERK-dependent phosphorylation as also observed in other studies [22, 42, 43].

We identified AURKA as a BIM-interacting protein, which lost interaction upon BIM phosphorylation. It has been reported that AURKA—in contrast to ERK—specifically phosphorylates BIM-EL during mitosis [44, 45]. Our mass spectrometry data however demonstrated that the interaction between unphosphorylated BIM and AURKA already drastically decreases upon steroid treatment. This decreased interaction might be caused by the downregulation of AURKA as a result of steroid treatment, as is observed in a BCP-ALL xenograft model [46]. Downregulation of AURKA in steroid-treated leukemia implies that AURKA does not actively contribute to steroid resistance, which would exclude AURKA inhibitors as therapeutic agents to reverse steroid resistance.

In addition to MAPK-ERK signaling, activation of the IL7R also leads to activation of the PI3K-AKT and JAK-STAT pathways, highlighting the complexity of IL7R signaling. Like MEK inhibitors, JAK and AKT inhibitors also seem promising to restore steroid sensitivity [28, 38]. Early T-cell progenitor (ETP) ALL patient cells are intrinsically more resistant to steroid treatment than non-ETP-ALL cells, frequently bear JAK-STAT activating mutations and are responsive to JAK1/2-inhibitor ruxolitinib [38]. Moreover, combination treatment of ruxolitinib and dexamethasone enhances steroid-induced cell death in IL7-dependent steroid resistant T-ALL cells due to IL7-induced JAK-STAT activation [29]. We confirm these findings and demonstrate that IL7-dependent steroid resistant T-ALL cells can benefit from synergistic effects of ruxolitinib on steroid-induced cytotoxicity in the presence of IL7. Moreover, we demonstrate that ruxolitinib also effectively blocks active MAPK-ERK signaling in IL7-dependent T-ALL PDX cells and JAK1 mutant T-ALL cells. The synergistic effect between JAK1/2-inhibition and steroids may therefore (in part) depend on the consequential inhibition of downstream MAPK-ERK signaling [38, 47].

With the exception of sample Z1808 that displays high STAT5 pathway activation in the absence of IL7 (i.e., IL7-induced signaling), we did not observe synergy between ruxolitinib and steroids in the remaining five IL7-dependent steroid resistant PDX samples in the absence of IL7. Our data suggests that the effect of ruxolitinib is limited to leukemic cells that utilize IL7-induced signaling to boost cell viability. In in-vivo PDX models that depend on active proliferation of leukemia cells, treatment with JAK1/2 inhibitors have been demonstrated to be effective and synergistic when combined with steroids. This effect might depend on the presence of stromal cells as main source for IL7 production. Our data however suggests the majority of non-proliferating cells will not respond to ruxolitinib treatment: (quiescent) leukemia cells in low-IL7-containing niches in patients may therefore not benefit from combined ruxolitinib and steroid treatment, limiting the curative application of ruxolitinib. This may be exemplified by the limited effect of ruxolitinib treatment in myeloproliferative neoplasms—a disease characterized by dominant mutational driven JAK-STAT pathway activation—since molecular remission upon ruxolitinib treatment is usually not achieved in these patients [48]. A similar dependency on IL7-enhanced viability is not a prerequisite for the synergistic effects of MEK inhibitors on steroid-induced cytotoxicity, and selumetinib was effective in all T-ALL PDX samples regardless of IL7-induced signaling. As the MAPK-ERK pathway is often activated downstream of active JAK-signaling, MEK inhibitors may provide a valuable alternative for ruxolitinib in JAK-STAT-activated neoplasms. Therefore, our data indicates that care should be taken implementing ruxolitinib in clinical practice for T-ALL.

In addition to our findings in T-ALL, the presence of RAS mutations in BCP-ALL at diagnosis predict for resistance to chemotherapeutic treatment and early relapse [49]. RAS mutations are enriched in relapsed BCP-ALL, frequently arising from minor subclones already present at diagnosis. MEK inhibitors also provide strong synergy with dexamethasone treatment in RAS-mutated BCP-ALL by enhancing functional BIM levels [50]. In addition, inhibition of the MAPK-ERK signaling cascade in ALL may enhance steroid sensitivity via the upregulation of p53 [51]. Results from these and other studies formed the basis of the phase I/II SeluDex trial (CT03705507) for mutant N/KRAS- (or FLT3, PTPN11 or cCBL) relapsed/refractory BCP-ALL and T-ALL patients [28, 50]. Our data indicates that JAK1 and IL7R α mutations could be included in the ‘RAS-activating mutations panel’ in the current SeluDex trial. As the MAPK-ERK pathway may represent a central junction for more signaling pathways than (mutant) IL7R-signaling, the effect of combined MEK inhibitor and steroid

treatment seems beneficial for a large group of T-ALL patients.

In conclusion, MAPK-ERK pathway inhibitors—and in particular MEK inhibitors—potentiate steroid-induced cell death by preventing the inactivation of (steroid-induced) pro-apoptotic BIM. Our data highlight the importance of MAPK-ERK signaling in T-ALL, since the synergistic effect of MEK inhibitors with steroids is not limited to IL7-induced signaling or the presence of specific activating (mutational) events. By expanding the inclusion criteria for the current SeluDex trial, the clinical effect of MEK inhibitors may be studied for more relapsed/refractory T-ALL patients to substantiate the potential use of combined MEK inhibitor and steroid therapy in future (first-line) treatment regimens.

Acknowledgements This study was sponsored by grants of the foundation “Kinderen Kankervrij”; KiKa-219 (JvdZ), KiKa-92, KiKa-295 (WKS), the Chemotherapy Foundation (AAF) and NIH grants P30 CA013696 (Flow Cytometry Shared Resource and Genomics Shared Resource, Herbert Irving Comprehensive Cancer Center) and R35 CA210065 (AAF). This research was part of the Netherlands X-omics Initiative and partially funded by NWO, project 184.034.019.

Author contributions JvdZ designed study, performed research and wrote paper. JBG, VC, DD, WKS, ZC and JD performed research. GZ, MA, KO, BB, J-PB, JC and AAF performed research, and provided critical input. JV, RP and BV provided critical input and wrote paper. JM designed and supervised the study and wrote paper.

Funding JV and BV: Cancer Research United Kingdom alliance funding from AstraZeneca for SeluDex trial (NCT03705507).

Compliance with ethical standards

Conflict of interest The authors declare no competing interests.

Publisher's note Springer Nature remains neutral with regard to jurisdictional claims in published maps and institutional affiliations.

References

- Pieters R, de Groot-Kruseman H, Van der Velden V, Fiocco M, van den Berg H, de Bont E, et al. Successful Therapy Reduction and Intensification for Childhood Acute Lymphoblastic Leukemia Based on Minimal Residual Disease Monitoring: study ALL10 From the Dutch Childhood Oncology Group. *J Clin Oncol*. 2016;34:2591–601.
- Conter V, Valsecchi MG, Parasole R, Putti MC, Locatelli F, Barisone E, et al. Childhood high-risk acute lymphoblastic leukemia in first remission: results after chemotherapy or transplant from the AIEOP ALL 2000 study. *Blood*. 2014;123:1470–8.
- Lauten M, Moricke A, Beier R, Zimmermann M, Stanulla M, Meissner B, et al. Prediction of outcome by early bone marrow response in childhood acute lymphoblastic leukemia treated in the ALL-BFM 95 trial: differential effects in precursor B-cell and T-cell leukemia. *Haematologica*. 2012;97:1048–56.
- Reedijk AMJ, Coebergh JWW, de Groot-Kruseman HA, van der Sluis IM, Kremer LC, Karim-Kos HE, et al. Progress against childhood and adolescent acute lymphoblastic leukaemia in the Netherlands, 1990-2015. *Leukemia*. 2021;35:1001–11.
- Kaspers GJ, Pieters R, Van Zantwijk CH, Van Wering ER, Van Der Does-Van Den Berg A, Veerman AJ. Prednisolone resistance in childhood acute lymphoblastic leukemia: vitro-vivo correlations and cross-resistance to other drugs. *Blood*. 1998;92:259–66.
- Lauten M, Stanulla M, Zimmermann M, Welte K, Riehm H, Schrappe M. Clinical outcome of patients with childhood acute lymphoblastic leukaemia and an initial leukaemic blood blast count of less than 1000 per microliter. *Klinische Padiatrie*. 2001;213:169–74.
- O'Connor L, Strasser A, O'Reilly LA, Hausmann G, Adams JM, Cory S, et al. Bim: a novel member of the Bcl-2 family that promotes apoptosis. *EMBO J*. 1998;17:384–95.
- Jing D, Bhadri VA, Beck D, Thoms JA, Yakob NA, Wong JW, et al. Opposing regulation of BIM and BCL2 controls glucocorticoid-induced apoptosis of pediatric acute lymphoblastic leukemia cells. *Blood*. 2015;125:273–83.
- Abrams MT, Robertson NM, Yoon K, Wickstrom E. Inhibition of glucocorticoid-induced apoptosis by targeting the major splice variants of BIM mRNA with small interfering RNA and short hairpin RNA. *J Biol Chem*. 2004;279:55809–17.
- Hall CP, Reynolds CP, Kang MH. Modulation of Glucocorticoid Resistance in Pediatric T-cell Acute Lymphoblastic Leukemia by Increasing BIM Expression with the PI3K/mTOR Inhibitor BEZ235. *Clin Cancer Res*. 2016;22:621–32.
- Ley R, Balmanno K, Hadfield K, Weston C, Cook SJ. Activation of the ERK1/2 signaling pathway promotes phosphorylation and proteasome-dependent degradation of the BH3-only protein, Bim. *J Biol Chem*. 2003;278:18811–6.
- Wang Z, Malone MH, He H, McColl KS, Distelhorst CW. Microarray analysis uncovers the induction of the proapoptotic BH3-only protein Bim in multiple models of glucocorticoid-induced apoptosis. *J Biol Chem*. 2003;278:23861–7.
- Wang C, Youle RJ. The role of mitochondria in apoptosis*. *Annu Rev Genet*. 2009;43:95–118.
- Willis SN, Fletcher JI, Kaufmann T, van Delft MF, Chen L, Czabotar PE, et al. Apoptosis initiated when BH3 ligands engage multiple Bcl-2 homologs, not Bax or Bak. *Science*. 2007;315:856–9.
- Gavathiotis E, Suzuki M, Davis ML, Pitter K, Bird GH, Katz SG, et al. BAX activation is initiated at a novel interaction site. *Nature*. 2008;455:1076–81.
- Piovan E, Yu J, Tosello V, Herranz D, Ambesi-Impiombato A, Da Silva AC, et al. Direct reversal of glucocorticoid resistance by AKT inhibition in acute lymphoblastic leukemia. *Cancer Cell*. 2013;24:766–76.
- Bachmann PS, Gorman R, Papa RA, Bardell JE, Ford J, Kees UR, et al. Divergent mechanisms of glucocorticoid resistance in experimental models of pediatric acute lymphoblastic leukemia. *Cancer Res*. 2007;67:4482–90.
- Bachmann PS, Piazza RG, Janes ME, Wong NC, Davies C, Mogavero A, et al. Epigenetic silencing of BIM in glucocorticoid poor-responsive pediatric acute lymphoblastic leukemia, and its reversal by histone deacetylase inhibition. *Blood*. 2010;116:3013–22.
- Singh A, Ye M, Bucur O, Zhu S, Tanya Santos M, Rabinovitz I, et al. Protein phosphatase 2A reactivates FOXO3a through a dynamic interplay with 14-3-3 and AKT. *Mol Biol Cell*. 2010;21:1140–52.
- Yang JY, Zong CS, Xia W, Yamaguchi H, Ding Q, Xie X, et al. ERK promotes tumorigenesis by inhibiting FOXO3a via MDM2-mediated degradation. *Nat Cell Biol*. 2008;10:138–48.
- Lu J, Quearry B, Harada H. p38-MAP kinase activation followed by BIM induction is essential for glucocorticoid-induced

- apoptosis in lymphoblastic leukemia cells. *FEBS Lett.* 2006;580:3539–44.
22. Hubner A, Barrett T, Flavell RA, Davis RJ. Multisite phosphorylation regulates Bim stability and apoptotic activity. *Mol Cell.* 2008;30:415–25.
 23. Leung KT, Li KK, Sun SS, Chan PK, Ooi VE, Chiu LC. Activation of the JNK pathway promotes phosphorylation and degradation of BimEL—a novel mechanism of chemoresistance in T-cell acute lymphoblastic leukemia. *Carcinogenesis.* 2008;29:544–51.
 24. Lei K, Davis RJ. JNK phosphorylation of Bim-related members of the Bcl2 family induces Bax-dependent apoptosis. *Proc Natl Acad Sci USA.* 2003;100:2432–7.
 25. Barata JT, Silva A, Brandao JG, Nadler LM, Cardoso AA, Boussiotis VA. Activation of PI3K is indispensable for interleukin 7-mediated viability, proliferation, glucose use, and growth of T cell acute lymphoblastic leukemia cells. *J Exp Med.* 2004;200:659–69.
 26. Ribeiro D, Melao A, van Boxtel R, Santos CI, Silva A, Silva MC, et al. STAT5 is essential for IL-7-mediated viability, growth, and proliferation of T-cell acute lymphoblastic leukemia cells. *Blood Adv.* 2018;2:2199–213.
 27. Silva A, Laranjeira AB, Martins LR, Cardoso BA, Demengeot J, Yunes JA, et al. IL-7 contributes to the progression of human T-cell acute lymphoblastic leukemias. *Cancer Res.* 2011;71:4780–9.
 28. Li Y, Buijs-Gladdines JG, Cante-Barrett K, Stubbs AP, Vroegindewij EM, Smits WK, et al. IL-7 Receptor Mutations and Steroid Resistance in Pediatric T cell Acute Lymphoblastic Leukemia: a Genome Sequencing Study. *PLoS Med.* 2016;13:e1002200.
 29. Delgado-Martin C, Meyer LK, Huang BJ, Shimano KA, Zinter MS, Nguyen JV, et al. JAK/STAT pathway inhibition overcomes IL7-induced glucocorticoid resistance in a subset of human T-cell acute lymphoblastic leukemias. *Leukemia.* 2017;31:2568–76.
 30. Meyer LK, Huang BJ, Delgado-Martin C, Roy RP, Hechmer A, Wandler AM, et al. Glucocorticoids paradoxically facilitate steroid resistance in T-cell acute lymphoblastic leukemias and thymocytes. *J Clin Investig.* 2020;130:863–76.
 31. Barata JT, Durum SK, Seddon B. Flip the coin: IL-7 and IL-7R in health and disease. *Nat Immunol.* 2019;20:1584–93.
 32. Erlacher M, Michalak EM, Kelly PN, Labi V, Niederegger H, Coultas L, et al. BH3-only proteins Puma and Bim are rate-limiting for gamma-radiation- and glucocorticoid-induced apoptosis of lymphoid cells in vivo. *Blood.* 2005;106:4131–8.
 33. Jing D, Huang Y, Liu X, Sia KCS, Zhang JC, Tai X, et al. Lymphocyte-Specific Chromatin Accessibility Pre-determines Glucocorticoid Resistance in Acute Lymphoblastic Leukemia. *Cancer Cell.* 2018;34:906–21. e8.
 34. Cheng EH, Wei MC, Weiler S, Flavell RA, Mak TW, Lindsten T, et al. BCL-2, BCL-X(L) sequester BH3 domain-only molecules preventing BAX- and BAK-mediated mitochondrial apoptosis. *Mol Cell.* 2001;8:705–11.
 35. Puthalakath H, Huang DC, O'Reilly LA, King SM, Strasser A. The proapoptotic activity of the Bcl-2 family member Bim is regulated by interaction with the dynein motor complex. *Mol Cell.* 1999;3:287–96.
 36. Gomez-Bougie P, Bataille R, Amiot M. Endogenous association of Bim BH3-only protein with Mcl-1, Bcl-xL and Bcl-2 on mitochondria in human B cells. *Eur J Immunol.* 2005;35:971–6.
 37. Korfi K, Smith M, Swan J, Somerville TC, Dhomen N, Marais R. BIM mediates synergistic killing of B-cell acute lymphoblastic leukemia cells by BCL-2 and MEK inhibitors. *Cell Death Dis.* 2016;7:e2177.
 38. Maude SL, Dolai S, Delgado-Martin C, Vincent T, Robbins A, Selvanathan A, et al. Efficacy of JAK/STAT pathway inhibition in murine xenograft models of early T-cell precursor (ETP) acute lymphoblastic leukemia. *Blood.* 2015;125:1759–67.
 39. Gianfelici V, Chiaretti S, Demeyer S, Di Giacomo F, Messina M, La Starza R, et al. RNA sequencing unravels the genetics of refractory/relapsed T-cell acute lymphoblastic leukemia. Prognostic and therapeutic implications. *Haematologica.* 2016;101:941–50.
 40. Trinquand A, Tanguy-Schmidt A, Ben Abdelali R, Lambert J, Beldjord K, Lengline E, et al. Toward a NOTCH1/FBXW7/RAS/PTEN-based oncogenetic risk classification of adult T-cell acute lymphoblastic leukemia: a Group for Research in Adult Acute Lymphoblastic Leukemia study. *J Clin Oncol.* 2013;31:4333–42.
 41. Richter-Pechanska P, Kunz JB, Hof J, Zimmermann M, Rausch T, Bandapalli OR, et al. Identification of a genetically defined ultra-high-risk group in relapsed pediatric T-lymphoblastic leukemia. *Blood Cancer J.* 2017;7:e523.
 42. Harada H, Quearry B, Ruiz-Vela A, Korsmeyer SJ. Survival factor-induced extracellular signal-regulated kinase phosphorylates BIM, inhibiting its association with BAX and proapoptotic activity. *Proc Natl Acad Sci USA.* 2004;101:15313–7.
 43. Biswas SC, Greene LA. Nerve growth factor (NGF) down-regulates the Bcl-2 homology 3 (BH3) domain-only protein Bim and suppresses its proapoptotic activity by phosphorylation. *J Biol Chem.* 2002;277:49511–6.
 44. Moustafa-Kamal M, Gamache I, Lu Y, Li S, Teodoro JG. BimEL is phosphorylated at mitosis by Aurora A and targeted for degradation by betaTrCP1. *Cell Death Differ.* 2013;20:1393–403.
 45. Gilley R, Lochhead PA, Balmanno K, Oxley D, Clark J, Cook SJ. CDK1, not ERK1/2 or ERK5, is required for mitotic phosphorylation of BIMEL. *Cell Signal.* 2012;24:170–80.
 46. Bhadri VA, Cowley MJ, Kaplan W, Trahair TN, Lock RB. Evaluation of the NOD/SCID xenograft model for glucocorticoid-regulated gene expression in childhood B-cell precursor acute lymphoblastic leukemia. *BMC Genom.* 2011;12:565.
 47. Verbeke D, Gielen O, Jacobs K, Boeckx N, De Keersmaecker K, Maertens J, et al. Ruxolitinib Synergizes With Dexamethasone for the Treatment of T-cell Acute Lymphoblastic Leukemia. *Hemisphere.* 2019;3:e310.
 48. Greenfield G, McPherson S, Mills K, McMullin MF. The ruxolitinib effect: understanding how molecular pathogenesis and epigenetic dysregulation impact therapeutic efficacy in myeloproliferative neoplasms. *J Transl Med.* 2018;16:360.
 49. Irving J, Matheson E, Minto L, Blair H, Case M, Halsey C, et al. Ras pathway mutations are prevalent in relapsed childhood acute lymphoblastic leukemia and confer sensitivity to MEK inhibition. *Blood.* 2014;124:3420–30.
 50. Matheson EC, Thomas H, Case M, Blair H, Jackson RK, Masic D, et al. Glucocorticoids and selumetinib are highly synergistic in RAS pathway mutated childhood acute lymphoblastic leukemia through upregulation of BIM. *Haematologica.* 2019;104:1804–11.
 51. Jones CL, Gearheart CM, Fosmire S, Delgado-Martin C, Evensen NA, Bride K, et al. MAPK signaling cascades mediate distinct glucocorticoid resistance mechanisms in pediatric leukemia. *Blood.* 2015;126:2202–12.